AIP | Applied Physics Letters

A laser-driven nanosecond proton source for radiobiological studies

Jianhui Bin, Klaus Allinger, Walter Assmann, Günther Dollinger, Guido A. Drexler et al.

Citation: Appl. Phys. Lett. **101**, 243701 (2012); doi: 10.1063/1.4769372
View online: http://dx.doi.org/10.1063/1.4769372
View Table of Contents: http://apl.aip.org/resource/1/APPLAB/v101/i24
Published by the American Institute of Physics.

A laser-driven nanosecond proton source for radiobiological studies

Jianhui Bin,[1,2] Klaus Allinger,[1,2] Walter Assmann,[1] Günther Dollinger,[3] Guido A. Drexler,[4] Anna A. Friedl,[4] Dieter Habs,[1] Peter Hilz,[1] Rainer Hoerlein,[2] Nicole Humble,[5] Stefan Karsch,[1,2] Konstantin Khrennikov,[2] Daniel Kiefer,[2] Ferenc Krausz,[1,2] Wenjun Ma,[1] Dörte Michalski,[5] Michael Molls,[5] Sebastian Raith,[1] Sabine Reinhardt,[1] Barbara Röper,[5] Thomas E. Schmid,[5] Toshiki Tajima,[1] Johannes Wenz,[2] Olga Zlobinskaya,[5] Joerg Schreiber,[1,2,a)] and Jan J. Wilkens[5,a)]

[1]*Faculty of Physics, Ludwig-Maximilians-Universität München, Am Coulombwall 1, 85748 Garching, Germany*
[2]*Max Planck Institute of Quantum Optics, Hans-Kopfermann-Str. 1, 85748 Garching, Germany*
[3]*Institut für Angewandte Physik und Messtechnik (LRT2), Universität der Bundeswehr München, Werner-Heisenberg-Weg 39, 85577 Neubiberg, Germany*
[4]*Department of Radiation Oncology, Ludwig-Maximilians-Universität München, Schillerstr. 42, 80336 München, Germany*
[5]*Department of Radiation Oncology, Technische Universität München, Klinikum rechts der Isar, Ismaninger Str. 22, 81675 München, Germany*

(Received 25 June 2012; accepted 5 September 2012; published online 10 December 2012)

Ion beams are relevant for radiobiological studies and for tumor therapy. In contrast to conventional accelerators, laser-driven ion acceleration offers a potentially more compact and cost-effective means of delivering ions for radiotherapy. Here, we show that by combining advanced acceleration using nanometer thin targets and beam transport, truly nanosecond quasi-monoenergetic proton bunches can be generated with a table-top laser system, delivering single shot doses up to 7 Gy to living cells. Although in their infancy, laser-ion accelerators allow studying fast radiobiological processes as demonstrated here by measurements of the relative biological effectiveness of nanosecond proton bunches in human tumor cells. © *2012 American Institute of Physics*. [http://dx.doi.org/10.1063/1.4769372]

Owing to their superior depth-dose profile, protons (or more generally ions) are a favorable choice in radiation therapy for cancer. Due to the high cost of conventional accelerators such as cyclotrons or synchrotrons, only a small number of ion beam facilities are in use world-wide. Laser-driven ion acceleration offers a potentially more compact and cost-effective means of delivering ion beams for radiotherapy.[1–3] This technology gained increasing interest recently, especially since proton energies beyond 50 MeV were realized experimentally.[4] However, the laser systems used to obtain these energies were rather large (typically with footprint areas of hundreds of square meters) with pulse energies of 20–500 J and were limited to single laser shots every 10–20 min. Nowadays, table-top femtosecond lasers with a repetition rate of 10 Hz and pulse energy of several J are available and continuously developing. By using such small and economic lasers, maximum proton energies of up to 40 MeV[5–8] have been achieved. Recently emerged new acceleration mechanisms like radiation pressure acceleration[3,9] predict higher ion energies and more efficient energy conversion from laser photons to ion kinetic energy.

Before clinical application of laser-driven ions can be considered, cell irradiation experiments with laser-driven beams[7,10–12] constitute an important preliminary step to demonstrate the increasing maturity of this technology. In addition, the biological effectiveness of ultrashort-pulsed beams with nanosecond ion bunches of high charge compared to quasi-continuous beams from conventional accelerators can be assessed. In a more general context, time-resolved radiobiological studies with sub-nanosecond particle bunches might help to elucidate the ultrafast processes underlying the biological response of cells to ion irradiation.[13] Here, we present a method to irradiate cells with truly nanosecond quasi-monoenergetic proton bunches with single shot doses of several Gy driven by a table-top high-power laser. This is in contrast to previous biological experiments with laser-driven beams that either used much broader energy spectra[7,10,12] or that had to accumulate 10–20 shots over a few seconds or longer in order to obtain relevant doses above 1 Gy.[7,10,11]

Our experiments were performed using the ATLAS laser at Max-Planck-Institute for Quantum Optics in Garching. The ATLAS laser is a table-top (~15 m^2) multi-TW Ti:Sapphire laser system based on chirped pulse amplification (CPA) delivering pulses with a duration of ~30 fs (full width at half maximum, FWHM) at 795 nm central wavelength. The typical intensity contrast is 10^{-5} at 2 ps before the peak of the pulse and was further enhanced to 10^{-8} utilizing a re-collimating double plasma mirror system with a reflectivity of 50% that is implemented in the laser. A 90° off-axis parabolic mirror (f/2) is used to focus the laser pulses with the remaining 0.4 J energy to a measured spot size of 3 μm FWHM diameter, yielding a peak intensity of 8×10^{19} W/cm^2, slightly lower than 1.2×10^{20} W/cm^2 for a perfect Gaussian beam. The experiments were performed in single shot mode. Diamond-like carbon (DLC) foils[14] with thicknesses of 20 and 40 nm were irradiated under normal incidence. Due to the co-moving nature of the ion dynamics in these thin targets,[3] we obtained

a)Authors to whom correspondence should be addressed. Electronic addresses: joerg.schreiber@mpq.mpg.de and wilkens@tum.de.

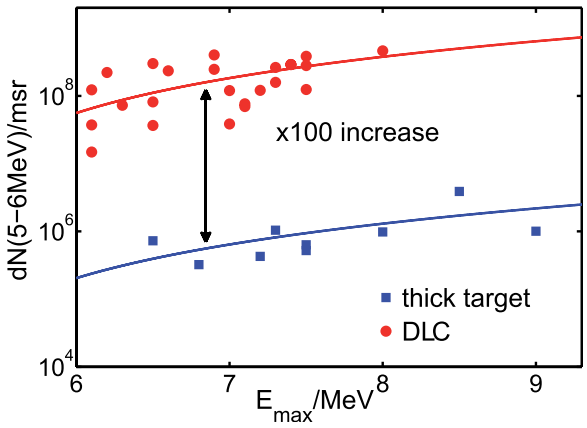

FIG. 1. Proton numbers per msr for nm-thin DLC targets (red) and 5 μm thick titanium targets (blue) in the energy band 5-6 MeV as a function of the maximum energy E_{max} representing a measure for performance of the setup at the ATLAS laser.

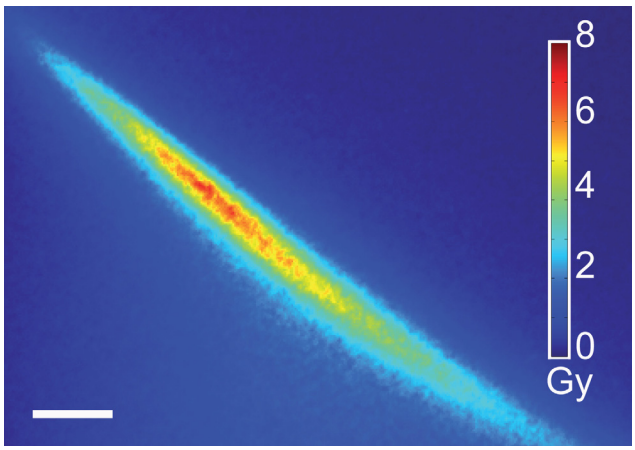

FIG. 3. Lateral dose distribution at the position of the cell sample measured with radiochromic film (maximum: 7.1 Gy in a single laser shot). Horizontal scale bar, 1 mm.

a hundred-fold higher proton fluence with 0.4 J laser energy compared to standard target normal sheath acceleration where 5 μm thick titanium foils and twice the laser energy were used (without plasma mirror; p-polarization; angle of incidence 45°). The maximum proton energy E_{max} of the broad spectrum remains similar in both cases. However, the number of protons accelerated to energies between 5 and 6 MeV in a solid angle of 1 msr, which can be easily transported with our quadrupole setup, is significantly increased by a factor of 100 (Fig. 1).

The technical setup of our beamline is illustrated in Fig. 2. A miniature quadrupole (QP) doublet composed of permanent magnets[15] with an aperture of 5 mm is inserted to focus protons with 5.2 MeV at a distance of 1.2 m. The first QP with a length of 36.0 mm and field gradient of 433 T/m was placed 12.4 mm behind the DLC foil, the second QP with length of 17.0 mm and a gradient of 505 T/m was separated by 7.7 mm. A circular aperture with 9 mm diameter was introduced 810 mm away from the target in front of a 100 mm long dipole magnet with 580 mT to deflect the proton bunch downwards. This avoids irradiation of the cell samples by X- or gamma-rays originating from the laser-target interaction, which cannot be shielded along the direct line of sight to the target. Our radiation monitors outside of the target chamber recorded such radiation, although suppressed by more than one order of magnitude compared to thick foil experiments. By removing the quadrupoles, which were mounted on motorized stages, the setup served as a proton spectrometer allowing optimization of the proton beam to achieve highest energies. A typical spectrum obtained by this procedure is displayed in Fig. 2. After the quadrupoles were inserted again, the setup produced an elliptical focus in the plane of the cells (1230 mm away from the target) with half axes of 0.45 mm and 5.2 mm at 50% of the maximum dose (Fig. 3) rotated by 40° with respect to the horizontal plane. The dose distribution was measured using self-developing radiochromic film[16] (Gafchromic EBT2). See supplementary material[23] for details of film dosimetry. The complete setup was tested for functionality at the Munich tandem accelerator (Maier Leibnitz Laboratory) employing a continuous beam of 9.8 MeV protons prior to implementation in the laser beamline.

The imaging properties of the complete setup including the quadrupoles, aperture and dipole magnet were calculated via a Monte-Carlo simulation revealing the design energy of 5.2 MeV in agreement with independent range measurements performed on the line focus. See supplementary material[23] for details of proton transport simulations. Due to the chromaticity of the quadrupoles, the initially broad energy distribution measured without the quadrupoles narrows over propagation as depicted by normalized spectra at different positions in Fig. 2. At the plane of the cells, half the protons are contained within a band of 0.3 MeV. This results in a difference in time of flight of ~1 ns, which determines the proton bunch duration as it is much longer than the 30 fs laser pulse. Under best conditions, we achieved a maximum proton fluence of $5.1 \times 10^6\,\mathrm{mm}^{-2}$ (mean fluence over the area of the line focus within 50% of maximum dose: $3.3 \times 10^6\,\mathrm{mm}^{-2}$) in a single shot, which corresponds to a maximum (mean) dose of 7.1 Gy (4.6 Gy) at the position of the cells. The maximum dose amounts to a peak dose rate of 7×10^9 Gy/s over an interval of 1 ns.

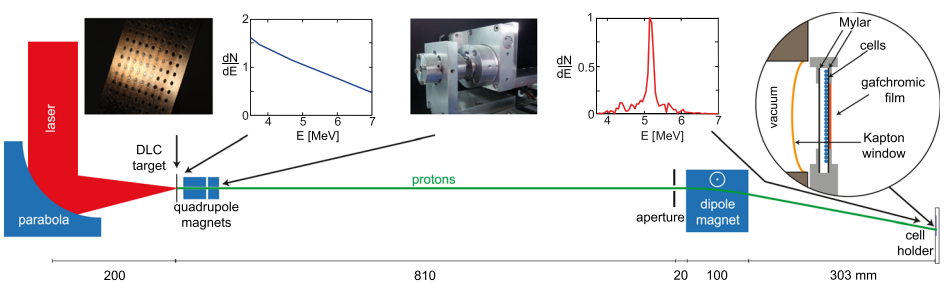

FIG. 2. Setup (to scale) of the laser-driven proton beamline. Protons accelerated from nm-thin foils are collimated by miniature quadrupoles in a small energy band. A dipole magnet deflects the beam downwards. Protons exit the vacuum chamber and enter the biological sample. The proton spectra are normalized to 1 for the design energy of 5.2 MeV.

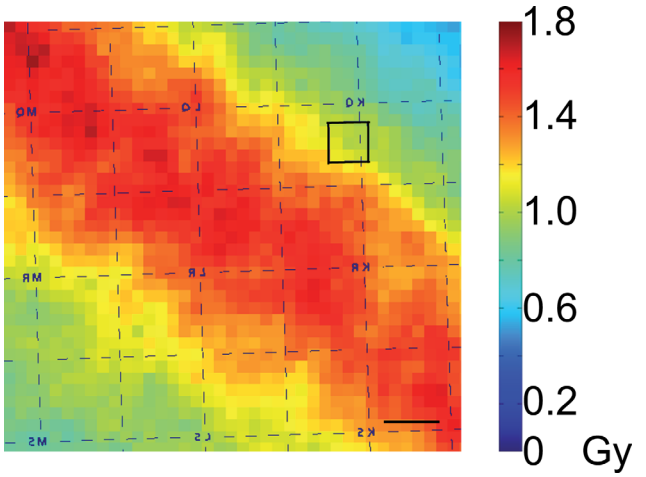

FIG. 4. Registration of the dose distribution measured by radiochromic film with the microstructured grid on the Mylar foil holding the cells. The exact location of the region of interest shown in Fig. 5(a) is indicated. Horizontal scale bar, 100 μm.

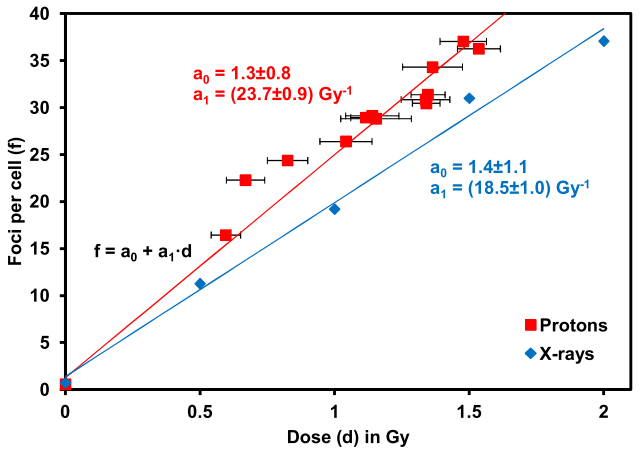

FIG. 6. Mean number of γ-H2AX foci per cell as a function of dose for laser-driven protons and 200 kV X-rays. Each data point for protons contains ~20 cells. Error bars in dose show the dose inhomogeneity (standard deviation) across the regions of interest used for evaluation.

To irradiate living cells in radiobiological experiments, the proton bunch leaves the vacuum through a 50 μm thick Kapton window and enters a customized cell holder. The Kapton foil was thick enough to completely stop a potential contribution of low-energy carbon ions which—if present in the primary beam at all—would be focused to the same point as 5.2 MeV protons depending on their charge and energy (e.g., C^{6+} ions with 1.3 MeV/u). Monolayers of human cervical cancer cells (HeLa) were exposed to protons generated in a single shot (mean energy at the position of the cells: 4.45 MeV), while the dose distribution was measured by radiochromic film placed immediately behind the cells (see supplementary material[23] for details on the irradiation setup and cell handling). By means of a microstructured grid on the cell holder and predefined marks on the film, the dose distribution can be spatially registered to microscopic images of the cells (Fig. 4). Customized image processing tools in MATLAB (The MathWorks, Inc.) allowed a registration with a spatial uncertainty of ± 1 pixel of the scanned film (21 μm).

The biological response in terms of initial damage to the deoxyribonucleic acid (DNA) was quantified using the γ-H2AX assay[17] (fixation: 30 min after irradiation). Double-strand breaks in the DNA are followed by a rapid phosphorylation of the histone H2AX, leading to a local concentration of the phosphorylated form (γ-H2AX) at the damaged site. Since this assay works best for doses below 2 Gy (otherwise the number of foci becomes too large to differentiate and count them individually), biological results are presented here for a cell sample exposed to a maximum dose of 1.7 Gy in a single shot. Fig. 5(a) shows some of the cells of this sample (exposed with a mean dose of 1.0 Gy across the depicted region, see Fig. 4), along with an unirradiated control sample (Fig. 5(b)). The bright red spots are foci of γ-H2AX visualized with specific antibodies labeled with a fluorescent dye.

The inhomogeneous dose distribution across the line focus in combination with the precise spatial registration of the delivered dose and the position of each cell allowed us to obtain full dose response curves for each irradiated sample in a single shot. An example is shown in Fig. 6, where the mean number of foci per cell (determined according to Ref. 18) is plotted against the mean dose for various regions of interest (142 × 106 μm^2) across the area of the line focus. Each data point is the mean over ~20 cells (total: 273 cells from the same sample). Horizontal error bars show the standard deviation of the dose values within each region (as a measure of the inevitable dose inhomogeneity due to the steep dose gradients). The uncertainty of ±1 pixel in the image registration leads to an additional uncertainty of ±4% in the mean dose value. Fig. 6 also gives a photon reference curve taken for the same cell line with 200 kV X-rays (>150 cells per data point, ~1000 cells in total) and linear fits[19] to

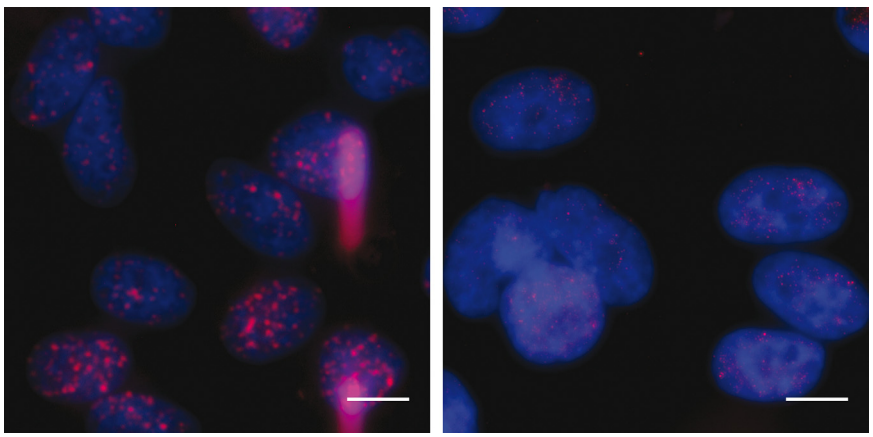

FIG. 5. Initial DNA damage in HeLa cells. (a) Sample exposed to a mean dose of 1.0 Gy and (b) corresponding unirradiated control. Foci of γ-H2AX (red) and cell nuclei (blue) are shown (3D microscopy, maximum intensity projections, background correction, contrast enhanced). The red vertical bars in (a) are part of the grid used for spatial registration (Fig. 4). Horizontal scale bars, 10 μm.

the data (least squares fit weighted with the number of cells in each data point). The slopes are 23.7 ± 0.9 foci per cell per Gy for protons and 18.5 ± 1.0 for X-rays. In both cases, sham-irradiated control samples showed only a low number of foci (on average 0.7 foci per cell). At an effect of 30 foci per cell (corresponding to an X-ray dose of 1.5 Gy), the relative biological effectiveness (RBE, defined as the ratio of X-ray dose and proton dose required to yield the same biological effect) for the induction of repair foci turned out to be 1.3 ± 0.3. The error estimate was determined by Gaussian error propagation of the uncertainties of the X-ray dose and proton dose values required for 30 foci per cell (X-ray dose uncertainty: $\pm 10\%$ according to the uncertainties in the fit parameters (Fig. 6) and $\pm 5\%$ in absolute dosimetry (systematic); proton dose uncertainty: $\pm 9\%$ according to the uncertainties in the fit parameters, $\pm 4\%$ for image registration (± 1 pixel), and $\pm 20\%$ in absolute dosimetry (systematic) including film calibration). This relatively large error is acceptable for a proof-of-principle experiment and will be reduced in subsequent experiments, mainly by improving the absolute proton dosimetry in the few MeV energy range.

The preliminary RBE obtained in this study is in agreement with proton RBE values in conventional beams at comparable proton energies[20] although measured for different biological endpoints. This indicates that no new radiobiological effects are to be expected for the distinctive combination of nanosecond proton delivery and single bunch dose rates of 10^9–10^{10} Gy/s as realized by our single bunch irradiation setup, even though it could equally be used for accumulated multi-bunch irradiations. This finding is in line with previous studies in single, nanosecond proton bunches at conventional sources,[21,22] and single or multiple ns bunches of laser-driven protons.[11,12] This confirms that for future applications in radiotherapy, where bunches of at least ns length (due to the propagation along an inevitable beamline of at least one meter between target and patient) and a maximum dose of a few Gy per shot will be applied, the same RBE as for conventional sources can be assumed.

By combining nanometer thin targets and proton beam optics we could demonstrate the potential of small, high repetition rate lasers for generating high proton yield, a nearly monoenergetic spectrum, and a reduction of background radiation (X- and gamma rays). Our method allows analyzing the full dose response to the nanosecond proton bunch attributed to a single laser pulse, enabling precise radiobiological experiments even in the presence of significant shot-to-shot fluctuations. By reducing the size of our setup further, proton bunches of sub-ns durations will be accessible for fundamental biological research soon. Although many issues still remain to be solved before clinical application becomes feasible, most importantly the progress towards higher ion energies much beyond 100 MeV per nucleon, we have demonstrated the feasibility of a very compact beamline for proton acceleration, transport, and delivery that future developments will build on.

Supported by DFG Cluster of Excellence: Munich-Centre for Advanced Photonics (MAP), by the International Max Planck Research School of Advanced Photon Science (IMPRS-APS), and by the Maier Leibnitz Laboratory of the Ludwig-Maximilians-Universität München and the Technische Universität München. We thank W. Carli, P. Foster, C. Greubel, F. Grüner, V. Hable, M. Hegelich, A. Henig, D. Jung, G. Rössling, S. Schell, T. Wenzl, M. Zepf, and the technical staff of the Munich tandem accelerator for their assistance.

[1]S. V. Bulanov and V. S. Khoroshkov, Plasma Phys. Rep. **28**, 453 (2002).
[2]C.-M. Ma, I. Veltchev, E. Fourkal, J. S. Li, W. Luo, J. Fan, T. Lin, and A. Pollack, Laser Phys. **16**, 639 (2006).
[3]T. Tajima, D. Habs, and X. Yan, Rev. Accel. Sci. Technol. **2**, 201 (2009).
[4]R. A. Snavely, M. H. Key, S. P. Hatchett, T. E. Cowan, M. Roth, T. W. Phillips, M. A. Stoyer, E. A. Henry, T. C. Sangster, M. S. Singh, S. C. Wilks, A. MacKinnon, A. Offenberger, D. M. Pennington, K. Yasuike, A. B. Langdon, B. F. Lasinski, J. Johnson, M. D. Perry, and E. M. Campbell, Phys. Rev. Lett. **85**, 2945 (2000).
[5]A. J. Mackinnon, Y. Sentoku, P. K. Patel, D. W. Price, S. Hatchett, M. H. Key, C. Andersen, R. Snavely, and R. R. Freeman, Phys. Rev. Lett. **88**, 215006 (2002).
[6]S. Fritzler, V. Malka, G. Grillon, J. P. Rousseau, F. Burgy, E. Lefebvre, E. d'Humières, P. McKenna, and K. W. D. Ledingham, Appl. Phys. Lett. **83**, 3039 (2003).
[7]S. D. Kraft, C. Richter, K. Zeil, M. Baumann, E. Beyreuther, S. Bock, M. Bussmann, T. E. Cowan, Y. Dammene, W. Enghardt, U. Helbig, L. Karsch, T. Kluge, L. Laschinsky, E. Lessmann, J. Metzkes, D. Naumburger, R. Sauerbrey, M. Schürer, M. Sobiella, J. Woithe, U. Schramm, and J. Pawelke, New J. Phys. **12**, 085003 (2010).
[8]K. Ogura, M. Nishiuchi, A. S. Pirozhkov, T. Tanimoto, A. Sagisaka, T. Z. Esirkepov, M. Kando, T. Shizuma, T. Hayakawa, H. Kiriyama, T. Shimomura, S. Kondo, S. Kanazawa, Y. Nakai, H. Sasao, F. Sasao, Y. Fukuda, H. Sakaki, M. Kanasaki, A. Yogo, S. V. Bulanov, P. R. Bolton, and K. Kondo, Opt. Lett. **37**, 2868 (2012).
[9]T. Esirkepov, M. Borghesi, S. V. Bulanov, G. Mourou, and T. Tajima, Phys. Rev. Lett. **92**, 175003 (2004).
[10]A. Yogo, K. Sato, M. Nishikino, M. Mori, T. Teshima, H. Numasaki, M. Murakami, Y. Demizu, S. Akagi, S. Nagayama, K. Ogura, A. Sagisaka, S. Orimo, M. Nishiuchi, A. S. Pirozhkov, M. Ikegami, M. Tampo, H. Sakaki, M. Suzuki, I. Daito, Y. Oishi, H. Sugiyama, H. Kiriyama, H. Okada, S. Kanazawa, S. Kondo, T. Shimomura, Y. Nakai, M. Tanoue, H. Sasao, D. Wakai, P. R. Bolton, and H. Daido, Appl. Phys. Lett. **94**, 181502 (2009).
[11]A. Yogo, T. Maeda, T. Hori, H. Sakaki, K. Ogura, M. Nishiuchi, A. Sagisaka, H. Kiriyama, H. Okada, S. Kanazawa, T. Shimomura, Y. Nakai, M. Tanoue, F. Sasao, P. R. Bolton, M. Murakami, T. Nomura, S. Kawanishi, and K. Kondo, Appl. Phys. Lett. **98**, 053701 (2011).
[12]D. Doria, K. F. Kakolee, S. Kar, S. K. Litt, F. Fiorini, H. Ahmed, S. Green, J. C. G. Jeynes, J. Kavanagh, D. Kirby, K. J. Kirkby, C. L. Lewis, M. J. Merchant, G. Nersisyan, R. Prasad, K. M. Prise, G. Schettino, M. Zepf, and M. Borghesi, AIP Adv. **2**, 011209 (2012).
[13]V. Malka, J. Faure, and Y. A. Gauduel, Mutat. Res. **704**, 142 (2010).
[14]W. Ma, V. K. Liechtenstein, J. Szerypo, D. Jung, P. Hilz, B. M. Hegelich, H. J. Maier, J. Schreiber, and D. Habs, Nucl. Instrum. Methods Phys. Res. A **655**, 53 (2011).
[15]M. Schollmeier, S. Becker, M. Geißel, K. A. Flippo, A. Blažević, S. A. Gaillard, D. C. Gautier, F. Grüner, K. Harres, M. Kimmel, F. Nürnberg, P. Rambo, U. Schramm, J. Schreiber, J. Schütrumpf, J. Schwarz, N. A. Tahir, B. Atherton, D. Habs, B. M. Hegelich, and M. Roth, Phys. Rev. Lett. **101**, 055004 (2008).
[16]S. Devic, Phys. Med. **27**, 122 (2011).
[17]E. P. Rogakou, D. R. Pilch, A. H. Orr, V. S. Ivanova, and W. M. Bonner, J. Biol. Chem. **273**, 5858 (1998).
[18]O. Zlobinskaya, G. Dollinger, D. Michalski, V. Hable, C. Greubel, G. Du, G. Multhoff, B. Röper, M. Molls, and T. E. Schmid, Radiat. Environ. Biophys. **51**, 23 (2012).
[19]N. A. P. Franken, R. Ten Cate, P. M. Krawczyk, J. Stap, J. Haveman, J. Aten, and G. W. Barendsen, Radiat. Oncol. **6**, 64 (2011).
[20]M. Belli, F. Cera, R. Cherubini, M. Dalla Vecchia, A. M. I. Haque, F. Ianzini, G. Moschini, O. Sapora, G. Simone, M. A. Tabocchini, and P. Tiveron, Int. J. Radiat. Biol. **74**, 501 (1998).
[21]T. E. Schmid, G. Dollinger, A. Hauptner, V. Hable, C. Greubel, S. Auer, A. A. Friedl, M. Molls, and B. Röper, Radiat. Res. **172**, 567 (2009).
[22]S. Auer, V. Hable, C. Greubel, G. A. Drexler, T. E. Schmid, C. Belka, G. Dollinger, and A. A. Friedl, Radiat. Oncol. **6**, 139 (2011).
[23]See supplementary material at http://dx.doi.org/10.1063/1.4769372 for details on film dosimetry, proton transport simulations, and the irradiation setup and cell handling.